Energy &
Environmental Science

Dynamic Article Links

Cite this: DOI: 10.1039/c2ee22019a

www.rsc.org/ees

PAPER

Worldwide health effects of the Fukushima Daiichi nuclear accident†

John E. Ten Hoeve[a] and Mark Z. Jacobson*[b]

Received 23rd April 2012, Accepted 26th June 2012
DOI: 10.1039/c2ee22019a

This study quantifies worldwide health effects of the Fukushima Daiichi nuclear accident on 11 March 2011. Effects are quantified with a 3-D global atmospheric model driven by emission estimates and evaluated against daily worldwide Comprehensive Nuclear-Test-Ban Treaty Organization (CTBTO) measurements and observed deposition rates. Inhalation exposure, ground-level external exposure, and atmospheric external exposure pathways of radioactive iodine-131, cesium-137, and cesium-134 released from Fukushima are accounted for using a linear no-threshold (LNT) model of human exposure. Exposure due to ingestion of contaminated food and water is estimated by extrapolation. We estimate an additional 130 (15–1100) cancer-related mortalities and 180 (24–1800) cancer-related morbidities incorporating uncertainties associated with the exposure–dose and dose–response models used in the study. We also discuss the LNT model's uncertainty at low doses. Sensitivities to emission rates, gas to particulate I-131 partitioning, and the mandatory evacuation radius around the plant are also explored, and may increase upper bound mortalities and morbidities in the ranges above to 1300 and 2500, respectively. Radiation exposure to workers at the plant is projected to result in 2 to 12 morbidities. An additional ~600 mortalities have been reported due to non-radiological causes such as mandatory evacuations. Lastly, a hypothetical accident at the Diablo Canyon Power Plant in California, USA with identical emissions to Fukushima was studied to analyze the influence of location and seasonality on the impact of a nuclear accident. This hypothetical accident may cause ~25% more mortalities than Fukushima despite California having one fourth the local population density due to differing meteorological conditions.

[a]*Department of Civil and Environmental Engineering, Stanford University, Yang and Yamazaki Environment and Energy Building, 473 Via Ortega, #390A, Stanford, California 94305-4020, USA. E-mail: tenhoeve@stanford.edu; Tel: +1 (650) 721-2730*
[b]*Department of Civil and Environmental Engineering, Stanford University, Yang and Yamazaki Environment and Energy Building, 473 Via Ortega, #397, Stanford, California 94305-4020, USA. E-mail: jacobson@stanford.edu; Tel: +1 (650) 723-6836*

† Electronic supplementary information (ESI) available. See DOI: 10.1039/c2ee22019a

Introduction

On 11 March 2011, a 9.0 magnitude earthquake and subsequent tsunami occurred off the Oshika Peninsula of Tōhoku Japan, causing widespread loss of life and property.[1] The tsunami inundated the Fukushima Daiichi Nuclear Power Station in northeastern Japan, causing a significant meltdown of nuclear fuel rods along with multiple explosions of hydrogen gas in three reactors after diesel backup cooling systems failed. Uranium fuel

Broader context

This study provides first estimates of the worldwide health impacts of the Fukushima nuclear accident. Because of the significant number of current nuclear power plants and their potential increase in the future, quantification of the health impacts from Fukushima is important. We find that inhalation exposure, external exposure, and ingestion exposure of the public to radioactivity may result in 15 to 1300 cancer mortalities and 24 to 2500 cancer morbidities worldwide, mostly in Japan. Exposure of workers to radioactivity at the plant is projected to result in another 2 to 12 cancers cases. This radiological health effect compares with the ~600 non-radiological deaths already attributed to the evacuation following the accident. Sensitivities of the estimated health effect to emission rates, gas to particle partitioning, and the mandatory evacuation radius around the plant are also calculated. Mortalities from Fukushima may be less than Chernobyl by much more than an order of magnitude due to a lower total emission of radioactivity, lower radioactivity deposition rates over land, and more precautionary measures taken immediately following the Fukushima accident. Lastly, a hypothetical accident at the Diablo Canyon Power Plant in California, USA is simulated to study the impact of meteorology on another coastal nuclear accident.

rods in the reactor #4 spent fuel pool also lost their cooling. Radiation from the crippled reactors began to leak no later than 12 March 2011.[2] The radiation release poisoned local water and food supplies and created a dead-zone of several hundred square kilometers around the site that may not be safe to inhabit for decades to centuries.[3] Some radiation was also transported long distances, and was detected as far away as North America and Europe.[4,5] Although emissions after a month were orders of magnitude lower than during the first few days, minimal releases continued until a total cold shutdown of the plant was achieved in December 2011.[6]

Several studies have tracked the emission, transport, and deposition of radionuclides from Fukushima using observational datasets and chemical transport models.[1,4,7–11] Initial studies have suggested that less than one quarter of the radioactivity was deposited over land in Japan, and only 1% of the radiation reached Europe.[4] However, no study to date has examined the global health effects of such radioactivity or simulated the radioactivity with a model that treats size-resolved aerosol particle microphysics or gas–aerosol–cloud interactions. Here, we used the GATOR-GCMOM global model to simulate the emissions, advection, decay, dissolution, aerosol–aerosol coagulation, aerosol–cloud coagulation, aerosol nucleation scavenging, rainout, washout, and dry deposition of radionuclides from the Fukushima Daiichi nuclear accident.[12,13] Atmospheric and ocean circulation, clouds, precipitation, aerosol processes, cloud processes, aerosol–cloud interactions, air–surface interactions, and radiation were all treated online in the model.[13] Results were evaluated against daily worldwide Comprehensive Nuclear-Test-Ban Treaty Organization (CTBTO) airborne radionuclide concentrations and deposition rates from around Japan.[14,15] Atmospheric and ground concentrations of iodine-131 (I-131), cesium-137 (Cs-137) and cesium-134 (Cs-134) were then used to estimate the worldwide health effects from the radioactive fallout.

Previous studies have modeled the dispersion and health effects of radioactive plumes from the Chernobyl nuclear accident.[16–20] Some of these studies have attributed thousands of cancer-related mortalities in Europe and Asia to the accident from a combination of acute and low-dose radiation exposure.[16,18,19] An increase in thyroid cancer attributed to the Chernobyl accident has been found in children and adolescents living in highly contaminated areas and an increase in leukemia has been detected among recovery and clean-up workers.[16] Overall, radioactive emissions from Fukushima were roughly an order of magnitude lower than from Chernobyl.[3] In addition, over 80% of the radioactivity from Fukushima was advected over the Pacific Ocean whereas the radioactivity from Chernobyl was largely deposited over land. Furthermore, collective radiation exposure to workers and local populations appears to be lower from Fukushima compared with Chernobyl due to stricter safety precautions taken after the Fukushima accident.[21–23] For these reasons, some have suggested that radiation exposure from the Fukushima nuclear accident had no health effects.[24,25] This contention is evaluated here.

Inhaled or ingested I-131 at low doses becomes localized in the thyroid gland increasing the risk of latent thyroid cancer and other thyroid diseases, whereas inhaled or ingested Cs-137 becomes distributed in soft tissues increasing the risk of various cancers.[26] A linear no-threshold (LNT) model of human exposure was used to calculate radiological health effects, similar to previous Chernobyl studies.[18,27,28] The LNT model assumes that each radionuclide disintegration has the same probability of causing cell transformation and that each transformed cell has the same probability of developing into a cancer. The LNT model has been employed extensively in the radiation safety and prevention communities,[27–30] yet some studies have questioned its validity at low doses[31–35] resulting in an ongoing debate.[36] Epidemiological studies have shown a statistically significant increase in stochastic cancer risk for doses above 100 mSv, however at doses below 100 mSv, significance or insignificance has not been demonstrated.[30] Similarly, linearity between dose and cancer risk has been detected for moderate doses with a lower bound of 45 mGy according to Japanese atomic bomb survivor data, but has not been demonstrated for low doses.[30,34] Some studies even suggest that low doses of ionizing radiation may instead be beneficial by stimulating immune response.[37] Yet, supporters of the LNT model claim that the difficulty in detecting and attributing a small number of cancers to low doses in a large population does not necessarily indicate there is an absence of risk at these low doses.[38] The U.S. Nuclear Regulatory Commission (NRC) states "The radiation protection community conservatively assumes that any amount of radiation may pose some risk for causing cancer and hereditary effect, and that the risk is higher for higher radiation exposures. The LNT hypothesis is accepted by the NRC as a conservative model for determining radiation dose standards, recognizing that the model may overestimate radiation risk".[39] The United Nations Scientific Committee on the Effects of Atomic Radiation (UNSCEAR) also supports a non-threshold response of radiation-induced cancer development at low doses.[30] Future developments in the field of health physics may confirm or refute the LNT hypothesis at low doses, but currently the analysis here remains within the accepted standards of radiation health methodologies.

In addition to modeling the radioactive release from Fukushima Daiichi, this study also examines the impact of radioactive release with identical emissions to Fukushima from a hypothetical nuclear accident at the Diablo Canyon Nuclear Power Plant in Avila Beach, CA during the months of March and September. These simulations were conducted to study the impact of geographic location and seasonality on health effects of a nuclear accident in comparison with Fukushima. The Diablo Canyon nuclear plant uses pressurized water reactors (PWRs) rather than the boiling water reactors used at the Fukushima Daiichi plant, yet PWRs are also susceptible to meltdown if reactor cooling is not continuously applied after the insertion of control rods, such as during the Three Mile Island nuclear accident.[40] The Diablo Canyon plant is also situated near multiple fault lines, and a 20-year extension of the plant's operating lifetime beyond 2025 is currently in doubt until new seismic studies can be conducted.[41] If the plant receives its license renewal, the chance that it will be subject to an earthquake exceeding its "safe shutdown earthquake" level is 13%.[42] Furthermore, an inspection of the Diablo Canyon Power Plant by the U.S. NRC following the disaster at

Fukushima Daiichi found a series of problems that could impact the ability to respond to a Fukushima-like event, including a susceptibility of the diesel generators to common failures due to similarities in design and location and a lack of training on how to operate diesel generators in adverse conditions.[43] We chose Diablo Canyon due to its earthquake vulnerability; however, every nuclear plant is susceptible to natural disaster or terrorist attack to some degree.[42]

Methods

Estimating radionuclide emissions based on observations

Emission rates of I-131 and Cs-137 in the model were constrained by emission estimates based on inverse modeling of worldwide Comprehensive Nuclear-Test-Ban Treaty Organization (CTBTO) observed concentrations. The CTBTO is a network of over 80 radionuclide monitoring stations used to detect and quantify radioactive species from nuclear explosions as well as fission-based products from nuclear power plants.[14] Stations located in Japan, Alaska, California, Hawaii, and the Pacific Islands were used to estimate source strengths in Becquerels (Bq) on the majority of days following the accident. The data were provided by the U.S. National Data Center and the Zentralanstalt für Meteorologie und Geodynamik (ZAMG).[44] The ZAMG estimated I-131 emissions between 1×10^{14} and 1×10^{17} Bq per day and Cs-137 emissions between 1×10^{13} and 1×10^{16} Bq per day, which compare well with our estimates provided in Table 1. We estimate total I-131 (Cs-137) emissions as 6.53×10^{16} Bq (1.70×10^{16} Bq) during the month following the accident. Our estimates are generally conservative by a factor of two with respect to I-131 and in line with respect to Cs-137 compared with estimates made by the Japanese government, including the Nuclear and Industrial Safety Agency and the Japan Atomic Energy Agency.[11] The Japanese Nuclear Safety Commission estimated an emission of 1.5×10^{17} Bq of I-131 and 1.2×10^{16} Bq of Cs-137 between 12 March 2011 and 5 April 2011,[45] which was updated to 1.3×10^{16} Bq of Cs-137 by Chino *et al.* [2011].[46] The Nuclear and Industrial Safety Agency estimated an emission of 1.6×10^{17} Bq of I-131 and 1.5×10^{16} Bq of Cs-137 between 12 March 2011 and 16 March 2011. Winiarek *et al.* [2012] predicted a comparable total Cs-137 emission rate (1.2×10^{16} Bq) but a higher I-131 emission rate ($1.9–3.8 \times 10^{17}$ Bq) over 11 March 2011 to 26 March 2011 compared with our estimates.[47] Stohl *et al.* [2011] predicted a Cs-137 emission rate roughly twice our emission rate using a similar methodology incorporating dispersion modeling and CTBTO observations,[9] yet their estimate is higher than other published estimates.[11]

Table 1 Estimated I-131 and Cs-137 emission rates (Bq per day) from Fukushima Daiichi over the period 12 March 2011 to 12 April 2011. This emission profile is employed in all simulations. The last row denotes the total emissions (Bq) over the month-long simulation

Date	I-131 emissions (Bq per day)	Cs-137 emissions (Bq per day)
03/12/11	3.0×10^{15}	7.5×10^{13}
03/13/11	4.0×10^{15}	1.0×10^{14}
03/14/11–03/15/11	2.5×10^{16}	5.0×10^{15}
03/16/11–03/19/11	1.0×10^{15}	7.5×10^{14}
03/20/11–03/26/11	5.0×10^{14}	5.0×10^{14}
03/27/11–04/04/11	7.5×10^{13}	2.5×10^{13}
04/05/11–04/12/11	1.0×10^{13}	7.5×10^{12}
Total (Bq)	6.526×10^{16}	1.696×10^{16}

During CTBTO measurements, large volumes of air pass through high efficiency filter paper used to collect particles over a 24 hour period. After 24 hours, the radioactivity is measured by a high-resolution gamma detector.[48] Maximum CTBTO detection limits are specified as 5 μBq m^{-3} for I-131 and 10 μBq m^{-3} for Cs-137, however, the detection limit of I-131 may realistically extend to 10 μBq m^{-3}.[49] These filters measure only particle activity concentrations, and do not measure gas concentrations; therefore, total radioactive emission estimates based solely on CTBTO measurements are adjusted to account for gas plus particle emissions using the method described in the following paragraph.

Environmental Protection Agency (EPA) RadNet measurements were used to determine the fraction of total ambient gas plus particle radioactive I-131 that was in the gas phase in order to scale CTBTO I-131 particle measurements to total gas plus particle I-131 values for comparison with the model.[50] U.S. Environmental Protection Agency (EPA) RadNet observations provided both particle and gas + particle I-131 taken from 12 sensors around the United States in Dutch Harbor, AK, Juneau, AK, Nome, AK, Montgomery, AL, Anaheim, CA, San Bernardino, CA, Kauai, HI, Oahu, HI, Boise, ID, Guam, Saipan, and Las Vegas, NV during the first two weeks of the accident. The EPA performs both filter sampling to measure particles as well as air cartridge sampling to measure both particles and gases. Over all stations and observations, the mean ratio of gas + particle I-131 to particle I-131 was 5.28 with a relatively small standard error of 0.51. This value agrees closely with other studies.[10,51] Measured CTBTO I-131 particle concentrations were multiplied by this ratio to estimate CTBTO I-131 gas + particle concentrations.

Modeled wet and dry deposition rates of Cs-137 were compared with observed daily deposition rates collected around Japan,[15] as well as with results from previous chemical transport model simulations.[10] Deposition rates were collected by the Ministry of Education, Culture, Sports, Science, and Technology of Japan beginning a few days after the accident.

GATOR-GCMOM model description

GATOR-GCMOM simulates atmospheric and ocean circulation, clouds, precipitation, emissions, transport, deposition, chemistry, aerosol processes, radiation, and air–surface interactions.[12,13] Horizontal and vertical advection of grid-scale gases and aerosols were solved with a peak-preserving, mass-conserving advection algorithm.[52] Total (gas plus particle) I-131 was treated as a gas and Cs-137 and Cs-134 were treated as sized-resolved particle components.[53] Based on EPA RadNet measurements, 81% of ambient I-131 was detected in the gas phase and 19% was detected in the particle phase. Because (a) the bulk of I-131 was in the gas phase, (b) the half-life of I-131 (8.03 days) is the same whether it is in the gas or particle phase, and (c) some gas-to-particle conversion mechanisms and properties of

I-131 are uncertain, total gas plus particle I-131 was treated as a gas in the model.

Following emission, I-131 was subject to radioactive decay, loss to clouds and precipitation (based on dissolution in clouds and rain), loss to the ocean (based on non-equilibrium gas-ocean transfer equations), dry deposition to land, snow, and ice surfaces, advection, convection, molecular diffusion, and turbulent diffusion. A Henry's law constant of 0.08 mol kg^{-1} atm^{-1} at 298 K was assumed for I-131 for gas–cloud and gas–ocean dissolution.[54] In health effect calculations, the percentage of I-131 assumed to be in the gas and particle phases was varied to find the sensitivity of the final result to the all-gas assumption for I-131. In these sensitivity calculations, particle I-131 was scaled from particle Cs-137 according to the relative emission rates of I-131 to Cs-137.

Cs-137 and Cs-134 were assumed to exist exclusively as particle components.[51] For Cs-137, the model treated size-resolved emissions, radioactive decay (with a half-life of 30.1 years), horizontal and vertical advection, cloud drop and ice crystal activation, aerosol–aerosol coagulation, aerosol–hydrometeor coagulation, tracking of Cs-137 in hydrometeor particles from entry to precipitation, aerosol sedimentation, aerosol dry deposition, condensational and dissolutional growth/evaporation of gases onto aerosol particles, and internal aerosol chemistry and hydration of aerosol particles.[13,55] Cs-134 concentrations and deposition rates in each grid cell and time step were scaled from Cs-137 concentrations and deposition rates assuming a Cs-134 to Cs-137 activity ratio of 0.9. This ratio was based on CTBTO observations following Fukushima, and is higher than the value of 0.5–0.6 associated with the Chernobyl fallout.[4] Constant mass activity coefficients for I-131 (4.587495×10^{15} Bq g^{-1}) and Cs-137 (3.20722×10^{12} Bq g^{-1}) were used to convert between mass and activity concentrations. A geometric mean number particle diameter of 0.06 μm and a geometric standard deviation of 2.0 were used to construct a lognormal distribution, which was then discretized into 14 aerosol size bins.[56] This emission size distribution is in the range of radioactive particle size distributions from the Chernobyl disaster and contains particle sizes small enough to be carried long distances.[57] Three hydrometeor distributions of cloud liquid, ice, and graupel were also used, each with 30 discrete size bins.

Wet and dry deposition of radionuclides were treated online in the model and were evaluated against observations and previous studies. Equations used for wet and dry deposition can be found in Jacobson [2005].[53] Ground surface concentrations of I-131, Cs-137, barium-137m (Ba-137m, the radioactive progeny of Cs-137), and Cs-134 were calculated in space and time by solving eqn (1), where F_{dep} is the location-(i,j) and time-resolved (t) deposition rate, k is the decay rate, and r is the weathering removal rate. About 93.5% of Cs-137 disintegrates to the metastable isotope Ba-137m after releasing a beta particle, which in turn disintegrates to the stable isotope Ba-137 after releasing a gamma particle.[58] We use decay rates of 1.4395×10^{-6} s^{-1}, 7.3217×10^{-10} s^{-1}, 4.5268×10^{-3} s^{-1}, and 1.0652×10^{-8} s^{-1} for I-131, Cs-137, Ba-137m, and Cs-134, respectively.[27] The weathering removal rate for I-131 is estimated to be 1×10^{-6} s^{-1} and the weathering removal rate for Cs-134 and Cs-137 is estimated to be 5.73×10^{-7} s^{-1}.[59]

$$\frac{d[I-131]_{i,j,t}}{dt} = F_{dep-I-131_{i,j,t}} - (k_{I-131} + r_{I-131})[I-131]_{i,j,t-1}$$

$$\frac{d[Cs-137]_{i,j,t}}{dt} = F_{dep-Cs-137_{i,j,t}} - (k_{Cs-137} + r_{Cs-137})[Cs-137]_{i,j,t-1}$$

$$\frac{d[Ba-137m]_{i,j,t}}{dt} = 0.935k_{Cs-137}[Cs-137]_{i,j,t-1} - k_{Ba-137m}[Ba-137m]_{i,j,t-1}$$

$$\frac{d[Cs-134]_{i,j,t}}{dt} = F_{dep-Cs-134_{i,j,t}} - (k_{Cs-134} + r_{Cs-134})[Cs-134]_{i,j,t-1} \quad (1)$$

Model simulations

Simulations to assess the worldwide transport and removal of airborne radioactive plumes from the Fukushima Daiichi Nuclear Power Station (141.0322° E, 37.4230° N) were conducted for the period between 12Z, 12 March 2011 and 12Z, 12 April 2011. A global simulation with a horizontal resolution of 1.5° W/E × 1.5° N/S and a vertical resolution of 68 sigma-pressure levels was run. Fifteen of the model layers were in the bottom 1 km and radioactive emissions were added at about 15 m height to the lowest model layer. The model was initialized with Global Forecast Systems (GFS) meteorological data corresponding to the start of simulation with no model spin-up.[60] Airborne concentrations and deposition rates at the end of the month-long simulation were assumed to decrease exponentially to a near-zero concentration during the following 8.5 months until a cold shutdown of the plant was assumed to occur.[6]

A nested global-high-resolution-regional simulation was also run to analyze the impact of the 20 km evacuation radius around the plant, declared a day after the accident.[61] The high resolution simulation was initialized on 12Z, 12 March 2011 to the same time as the start of the global simulation. A horizontal resolution of 0.45° W/E × 0.36° N/S and a vertical resolution of 35 sigma pressure levels were used for the interior domain. Due to the large computational time of this nested simulation, only an 84 hour run was conducted. The 20 km evacuation radius extended partially into four high-resolution-simulation grid cells containing the Fukushima plant. We assumed a constant population density across each grid cell and distributed the fraction of the population within the 20 km evacuation radius equally into the 11 nearest grid cells with land. This scenario assumed that evacuees did not travel more than 130 km from the Fukushima power plant. We compared this scenario with an alternate evacuation scenario where the evacuees were equally distributed among the specific spots recommended for evacuation in Akahane *et al.* [2012].[23] These analyses provided only a rough estimate of the effect of the evacuation since the precise number of evacuees, the time at which evacuees relocated, and the exact location where evacuees relocated to were not well-known enough to draw firm conclusions.

To illustrate the effect of geographic location on the health impact of a nuclear accident, simulations were conducted for a hypothetical accident at the Diablo Canyon Power Plant

(120.8561° W, 35.2108° N). One simulation was initialized on the same day as the Fukushima simulation, 12 March 2011, and another was initialized on 12 September 2006 to study the effect of the background meteorology on results. In California, frequent winter storms stemming from the Aleutian Low occur during March. The Pacific High dominates the weather during the month of September, resulting in a shallow inversion layer and predominantly clear skies. In both simulations, radioactive emission rates over time were identical to those from the Fukushima Daiichi accident for the month-long simulation period. Airborne concentrations and deposition rates at the end of each simulation were assumed to decrease exponentially to a near-zero concentration during the following 8.5 months, similar to Fukushima.

Calculation of health effects

Inhalation exposure, ground-level external exposure, and atmospheric external exposure pathways were considered in this study for I-131, Cs-134, Cs-137, and Ba-137m. Exposure–dose relationships and dose–response relationships for each radionuclide were determined using the U.S. EPA Dose and Risk Calculation (DCAL) software.[27,62] The software provided organ-specific, age-specific, and gender-specific relative risk coefficients for the inhalation pathway. A dose and dose rate effectiveness factor of two was applied to all organ-specific risk coefficients except for the breast.[27,28] Organ-specific risk coefficients were then integrated over the body to obtain whole-body risk coefficients. Age- and gender-specific relative risk coefficients[62] and inhalation rates[27] were weighted by the age and gender distribution of each country and continent.[63] Material-specific deposition and absorption models from the lungs to the blood were contained within the inhalation relative risk coefficients and slow, medium, and fast absorption models were used to provide a range in the coefficients.[62] A dose and dose rate effectiveness factor of two was also applied to all whole-body external exposure relative risk coefficients. Radionuclide-specific uncertainties were assigned to all inhalation and external exposure relative risk coefficients according to sensitivity studies using different but equally plausible biokinetic and dosimetric models.[27] These uncertainties provided a relatively large range in the relative risk coefficients used in this study; however, these ranges are appropriate since many of the computed relative risk coefficients are not well established. For these ranges, the best estimate is near the geometric mean of the lower bound and upper bound estimates. For inhalation exposure, the maximum uncertainty range was provided given absorption model uncertainties and biokinetic model uncertainties, resulting in a larger health effect range for inhalation exposure compared with external exposure. Health effects from radionuclide ingestion pathways were not calculated in this study due to the additional complexities and uncertainties relating to international trade and human consumption of food and water. However, we roughly estimate the health effect from this pathway based on a previous study of the Chernobyl nuclear accident.[18]

The excess lifetime cancer mortality or morbidity risk due to the inhalation exposure pathway was determined from eqn (2), where y_s is the total number of lifetime cancer mortalities or morbidities due to species s over all times t and grid cells i,j, $P_{i,j}$ is the 2003 population in each grid cell i,j scaled to estimated 2010 values,[63] β_s is the relative cancer mortality or morbidity risk coefficient for species s expressed in units of Bq^{-1}, I is the inhalation rate, $x_{i,j,t,s}$ is the species concentration s in each grid cell i,j at time t, and $x_{th,s}$ is the threshold concentration below which no health effect occurs.[64] A minimum threshold value of zero was assigned to each radionuclide, in accordance with the LNT assumption. External ground-level and external atmospheric exposure were calculated using a similar equation without I and with β_s having units of $m^2\ Bq^{-1}\ s^{-1}$ or $m^3\ Bq^{-1}\ s^{-1}$. The effect of sheltering inside structures was also taken into account by assuming a 30% reduction in exposure from particulate Cs-137 and Cs-134 for 12 hours each day when people are assumed to be indoors.[65] We assume an average particle size of 1 μm and average air exchange rate and air filter removal efficiencies for typical buildings.[65]

$$y_s = \sum_i \sum_j \left\{ P_{i,j} \left[1 - \exp\left[-\beta_s \sum_t \left(I \max\left(x_{i,j,t,s} - x_{th,s}, 0 \right) \right) \right] \right] \right\} \quad (2)$$

Inhalation exposure, ground-level external exposure, and atmospheric external exposure health effects were calculated for all radionuclides using modeled air and ground concentrations over the month-long simulation. Between the end of the simulation and the assumed cold shutdown 8.5 months later, health effects for all radionuclides were calculated using estimated airborne concentrations and deposition rates. Between cold shutdown and the following 50 years, only ground-level exposure was calculated for Cs-137, Ba-137m, and Cs-134. Ground-level exposure from I-131 was assumed to be negligible after the 8.5 months following the simulation due to its short half-life. Mortality risk is defined as an estimate of the risk to an average member of the population of dying from cancer over their lifetime. Morbidity risk is the risk of experiencing radiogenic cancer during a person's lifetime, whether or not the cancer is fatal.

Results

Fukushima simulations

Fig. 1 compares CTBTO measured concentrations with modeled I-131 and Cs-137 concentrations for the first 20 days of the simulation. The figure shows relatively good agreement between modeled and observed concentrations for all eight stations pictured, although some under- and over-predictions are observed. For instance, concentrations were under-predicted on 17 March 2011–21 March 2011 at the closest station to the Fukushima nuclear plant, Takasaki, Japan, located 200 km to the southeast. The timing of the plume reaching most stations is predicted reasonably well, however. Radioactivity reached the west coast of North America roughly four days after the start of the simulation and reached the east coast of North America roughly seven days after the start of the simulation.

GATOR-GCMOM gaseous dry deposition rates have been validated against measurements in previous simulations. In a 10 year climate simulation using GATOR-GCMOM, the modeled worldwide H_2 dry deposition rate was calculated as 72.9 Tg per year. This value is in the range of estimates from other studies,

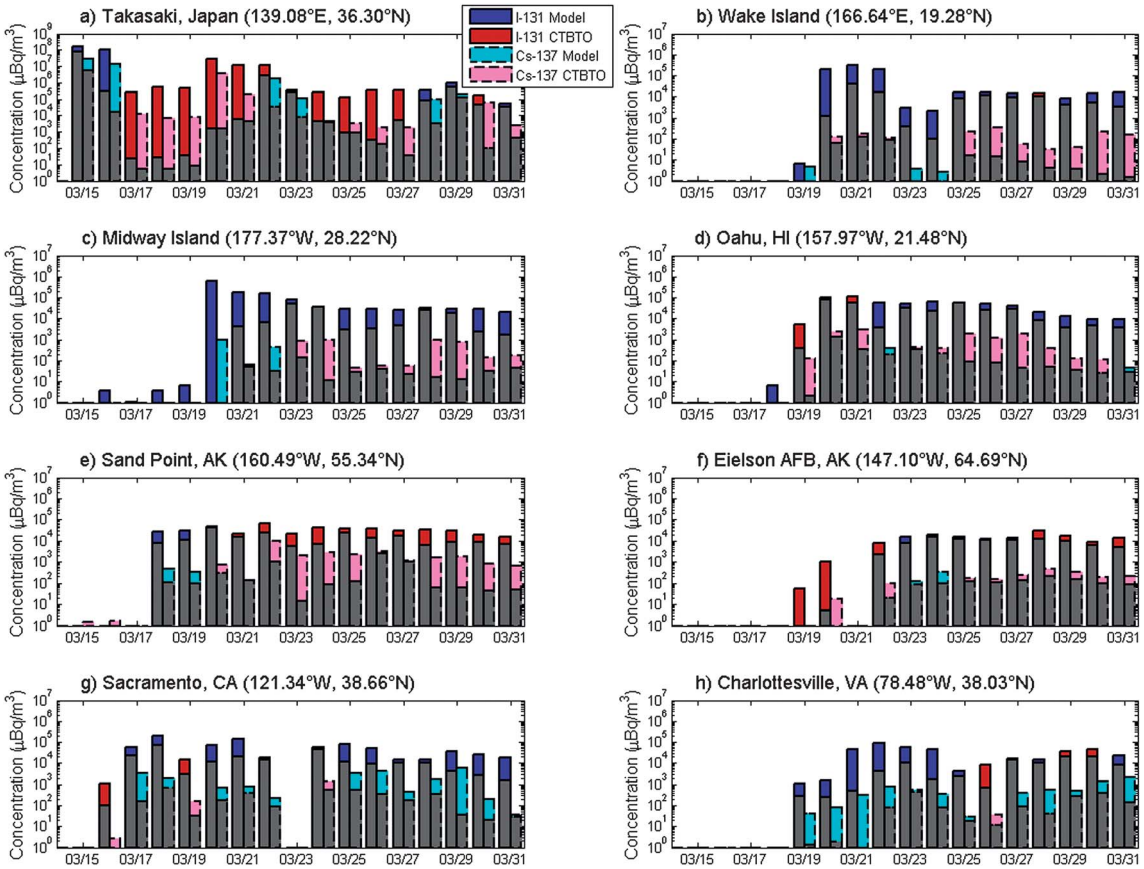

Fig. 1 Comparison between CTBTO activity concentration measurements and near-surface modeled activity concentrations (μBq m^{-3}) of I-131 (solid bars) and Cs-137 (dashed bars) for the first 20 days of the Fukushima Daiichi simulation at eight worldwide locations, (a)–(h). Dark blue and cyan colors represent an overestimate by the model for I-131 and Cs-137, respectively, and dark red and pink colors represent an underestimate by the model for I-131 and Cs-137, respectively. Grey represents overlap between observations and model results. Model results are not shown for days with missing CTBTO measurements. The same 24 h sampling window, ending on the stated day, was employed between observations and model results. No radioactivity was measured at any station before 15 March 2011.

56–90 Tg per year.[66–68] Wet deposition rates were validated using measured values of ground Cs-137 concentrations throughout Japan in the weeks following the Fukushima nuclear accident.[15] Fig. 2 shows dry, wet, and total deposition rates of Cs-137 over Japan during the one-month simulation period. Deposition rates near the accident (Fig. 2a and b) and farther downwind (Fig. 2c–f) were relatively consistent between the observations and the model. While inconsistencies between model results and observations occurred on several days, the timing of the precipitation events matched relatively well for most stations. The high deposition rates modeled on 15 March 2011–16 March 2011 in Fig. 2a–c, before observations were taken, were consistent with chemical transport model simulations from Morino *et al.* [2011].[10]

Fig. 3 shows a map of total Cs-137 deposition summed over the month-long simulation. Only 19% of total worldwide deposited Cs-137 was deposited over land areas while the remaining 81% was deposited over oceans. These percentages are in close agreement with Morino *et al.* [2011] who estimated that 22% of Cs-137 was deposited over land in Japan.[10] Fig. 4 shows time series of ground Cs-137 concentrations averaged over different regions. Ground concentrations were roughly an order of magnitude higher in Japan than in the United States, China, or Europe. Peak ground concentrations in Japan occurred on 15 March 2011–16 March 2011 when both emission rates and wet deposition rates were highest (Table 1 and Fig. 2). Other local maxima on 23 March 2011 and 26 March 2011 also corresponded to precipitation events. Peak ground concentrations in the United States occurred nearly two weeks later, on 28 March 2011.

Fig. 5 shows four snapshots of the I-131 plume throughout the simulation. The evolution of the Cs-137 plume is shown in Fig. 6. During the first 36 hours of simulation, the majority of radioactive emissions were advected eastward over the Pacific Ocean (Fig. 5a). A week into the simulation, radioactivity had spread throughout the Northern Pacific, reaching the contiguous United States, Alaska, and Russia (Fig. 5b). By the second week of the simulation, radioactivity had spread across the Atlantic but had not crossed the equator (Fig. 5c). By the third week of the simulation, radioactivity was relatively well-mixed throughout the Northern Hemisphere (NH). Population-weighted concentrations averaged over the NH increased to a maximum of 3 170 000 μBq m^{-3} for I-131 and 5 28 000 μBq m^{-3} for Cs-137 about two and a half days into the simulation. Average concentrations then decreased for the remainder of the month-long simulation to final values of 4100 μBq m^{-3} for I-131 and 260 μBq m^{-3} for Cs-137.

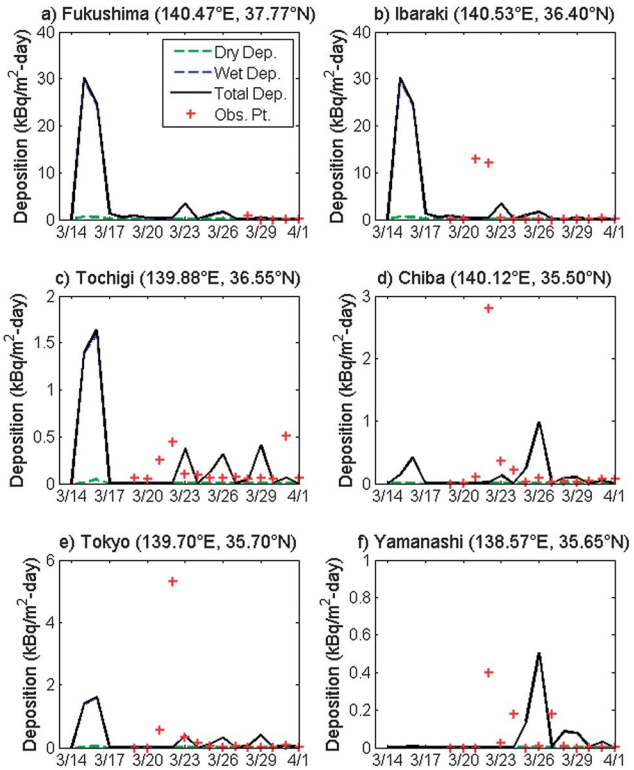

Fig. 2 Comparison between modeled dry, wet, and total deposition rates of Cs-137 activity and measured Cs-137 deposition rates for the first 20 days of the Fukushima Daiichi simulation at six locations across Japan (a)–(f). Observations began no earlier than 19 March 2011.

Table 2 indicates the range of excess mortality and morbidity due to radioactivity from Fukushima Daiichi by country, continent, and exposure pathway. The range in each table cell is derived from uncertainties in the assumed relative risk coefficients and not from uncertainties in emissions or model processes. The middle value in each range represents the best estimate. Two to three significant digits are provided to highlight differences between regions and pathways, but are not meant to imply the significance of the results. Also indicated in Table 2 is the percentage of mortalities and morbidities attributed to

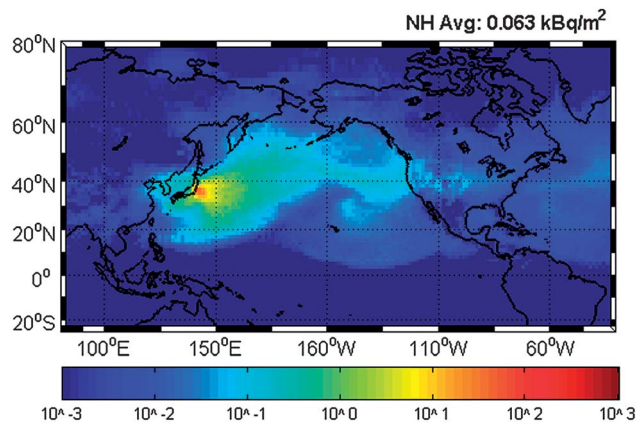

Fig. 3 Total wet + dry deposition of Cs-137 (kBq m^{-2}) summed over the one-month Fukushima Daiichi simulation. The Northern Hemisphere (NH) average noted above the figure is weighted by population.

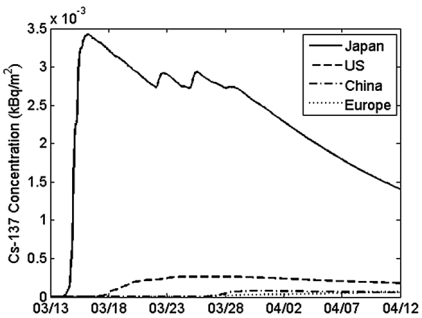

Fig. 4 Time series of Cs-137 ground concentrations (kBq m^{-2}) averaged over Japan, the United States, China, and Europe for the one-month Fukushima Daiichi simulation.

radioactivity between the end of the one-month simulation on 12 April 2011 and 50 years after the accident, including the 8.5 month period between the end of the one-month model simulation and the date the plant was assumed to achieve a cold shutdown.

The majority of the worldwide health effects occurred in Japan near the beginning of the simulation when emission rates were high. For other countries, the health impacts were much smaller. About 22% (27%) of the inhalation exposure and external exposure mortality (morbidity) was due to I-131, 21% (17%) was due to Cs-137 and Ba-137m, and 57% (56%) was due to Cs-134. The high percentage attributed to Cs-134 is due to its higher relative risk compared with Cs-137 and its longer half-life compared with I-131.[27] In sum, I-131, Cs-137 (and Ba-137m), and Cs-134 released from the Fukushima nuclear accident was estimated to result in 100 (14–950) worldwide excess cancer-related mortalities and 140 (23–1600) excess morbidities through inhalation, ground-level external exposure, and atmospheric external exposure combined.

These health impacts occurred in addition to radionuclide impacts on local water supplies, soils, agricultural crops, and livestock, which were not explicitly quantified here. A study of the Chernobyl nuclear accident suggested that between 50% and 90% of the external exposure + ingestion, 50 year health effects may have been due to external exposure.[18] Therefore, multiplying our low-end worldwide external exposure health effect by 1.1, our high-end worldwide external exposure health effect by 2.0, and our best guess external exposure health effect by 1.6 and adding these scaled estimates to the inhalation health effect provided a crude estimate of the total radiological health effect from Fukushima, accounting for all exposure pathways. Performing this extrapolation, we estimate 130 (15–1100) worldwide excess mortalities and 180 (24–1800) excess morbidities from all exposure pathways. A more detailed analysis of the ingestion exposure pathway is needed to better approximate total radiological health effects from Fukushima; however, we believe that a more accurate analysis will likely fall within the estimates provided here. Of total best estimate mortalities (morbidities), 48% (46%) was due to the inhalation exposure pathway, 33% (34%) was due to the ground-level exposure pathway, 19% (19%) was due to the ingestion pathway, and ~1% was due to the atmospheric exposure pathway. We also find that over 90% of total worldwide mortalitites and morbidities are projected to occur in Japan.

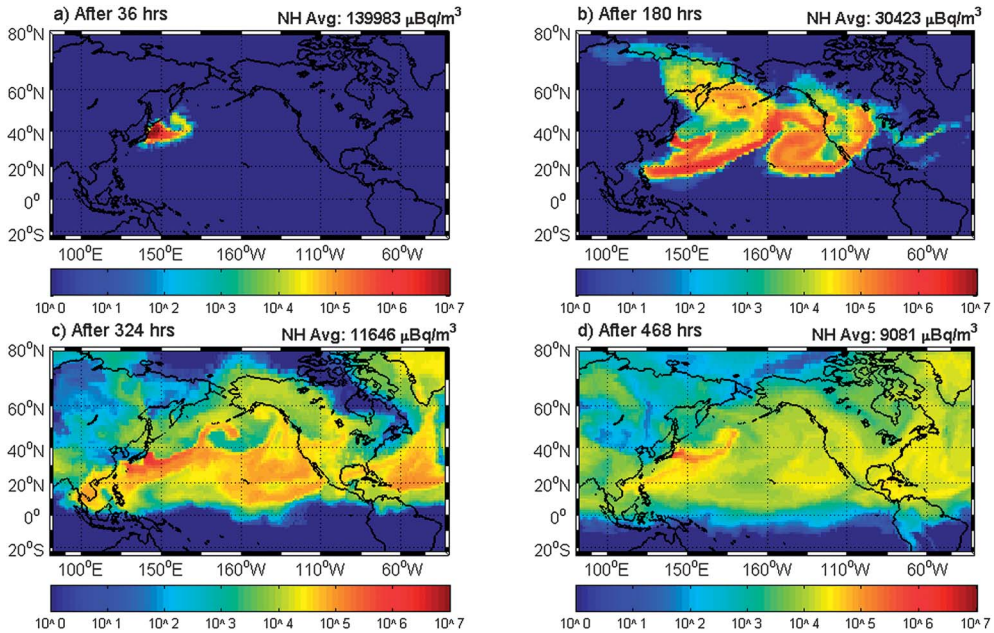

Fig. 5 Modeled near-surface atmospheric worldwide activity concentrations (μBq m^{-3}) of I-131 (a) 36 hours (1.5 days), (b) 180 hours (7.5 days), (c) 324 hours (13.5 days), and (d) 468 hours (19.5 days) into the Fukushima Daiichi simulation. Northern Hemisphere (NH) averages noted above each panel are weighted by population.

A 20 km evacuation radius around the plant was declared soon after the accident, adding uncertainty to the calculation of local health impacts. A high-resolution nested simulation was conducted for 84 hours over Japan to assess the effect of this evacuation radius. 22% fewer total mortalities and morbidities due to evacuation procedures were calculated assuming evacuees moved in equal proportions to neighboring grid cells. If evacuees were assumed to take shelter in the specific spots recommended for evacuation, the resulting health benefits were similar, 20% fewer mortalities and morbidities.[23] Yet, the lives saved due to the evacuation may be an overestimate since reports indicate that policymakers failed to evacuate people away from the plume immediately following the accident.[69]

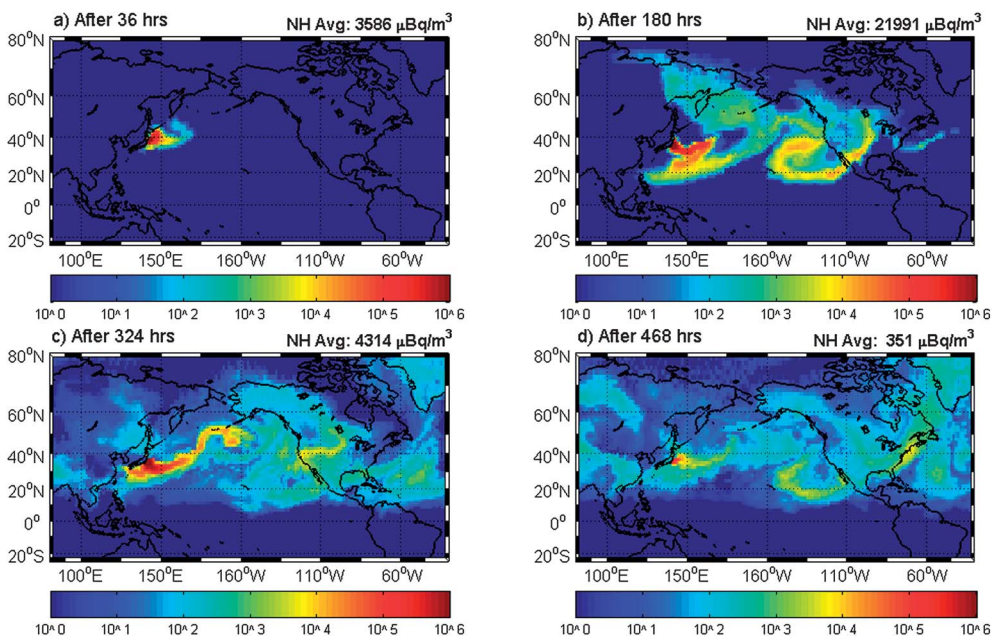

Fig. 6 Modeled near-surface atmospheric worldwide activity concentrations (μBq m^{-3}) of Cs-137 (a) 36 hours (1.5 days), (b) 180 hours (7.5 days), (c) 324 hours (13.5 days), and (d) 468 hours (19.5 days) into the Fukushima Daiichi simulation. Northern Hemisphere (NH) averages noted above each panel are weighted by population.

Table 2 Excess lifetime mortalities and morbidities from radioactivity released from Fukushima Daiichi by region. The middle value provides the best estimate and the upper and lower values provide the uncertainty in the health effect based on uncertainties in the biokinetic, dosimetric, and absorption models used. The "Percent Total After End Simulation" is the percent of mortalities or morbidities occurring in the 50 years following the one-month simulation, including the 8.5 month period between the end of the one-month simulation and when cold shutdown of the plant was assumed to occur. The final row provides an estimate of the total health effect including ingestion exposure extrapolated from Chernobyl estimates

	Mortalities					Morbidities				
	Inhalation exposure	Ground-level external exposure	Atmospheric external exposure	Total	Percent total after end simulation	Inhalation exposure	Ground-level external exposure	Atmospheric external exposure	Total	Percent total after end simulation
Asia	3.0–58–774	10–39–153	0.26–1.0–3.9	13–99–931	27	6.4–79–1280	15–58–224	0.39–1.5–5.8	22–139–1510	29
North America	0.04–0.61–5.6	0.20–0.76–2.9	0.00–0.01–0.05	0.24–1.4–8.6	48	0.10–1.0–17	0.29–1.1–4.3	0.00–0.02–0.07	0.39–2.1–22	46
Europe	0.02–0.27–2.4	0.16–0.61–2.4	0.00–0.00–0.03	0.17–0.89–4.8	76	0.05–0.45–7.6	0.23–0.89–3.5	0.00–0.01–0.04	0.28–1.4–11	75
Africa	0.02–0.33–3.0	0.06–0.22–0.84	0.00–0.00–0.02	0.08–0.55–3.8	61	0.05–0.57–10	0.08–0.32–1.2	0.00–0.00–0.03	0.14–0.90–12	59
Japan	2.9–57–761	9.3–36–140	0.25–0.99–3.8	13–94–905	25	6.2–77–1240	14–53–205	0.38–1.5–5.6	20–131–1450	27
China	0.03–0.50–4.5	0.43–1.7–6.5	0.00–0.01–0.04	0.47–2.2–11	69	0.08–0.81–14	0.64–2.5–9.6	0.00–0.02–0.07	0.72–3.3–23	68
South Korea	0.00–0.02–0.20	0.19–0.73–2.8	0.00–0.00–0.00	0.19–0.75–3.0	72	0.00–0.03–0.50	0.28–1.1–4.1	0.00–0.00–0.00	0.28–1.1–4.6	71
United States	0.02–0.40–3.7	0.17–0.66–2.5	0.00–0.00–0.03	0.20–1.1–6.3	51	0.06–0.65–11	0.25–0.96–3.7	0.00–0.01–0.05	0.32–1.6–15	49
Mexico	0.00–0.13–1.2	0.00–0.03–0.12	0.00–0.00–0.00	0.02–0.16–1.3	30	0.02–0.22–3.8	0.01–0.04–0.17	0.00–0.00–0.01	0.03–0.26–3.9	29
Canada	0.00–0.03–0.26	0.01–0.05–0.21	0.00–0.00–0.00	0.02–0.08–0.47	58	0.00–0.05–0.77	0.02–0.08–0.31	0.00–0.00–0.00	0.03–0.13–1.1	56
Worldwide	3.1–60–785	11–41–159	0.27–1.0–4.0	14–102–948	28	6.7–81–1320	16–60–234	0.40–1.5–6.0	23–143–1560	30
	Worldwide total mortality incl. ingestion			15–125–1110		Worldwide total morbidity incl. ingestion			24–178–1800	

Health effects were also found to be sensitive to the emission rate of I-131 and the treatment of I-131 as a gas or particle. If total I-131 emissions were doubled to 1.31×10^{17} Bq, an estimate more in line with others,[11] total mortalities from all exposure pathways would increase by 18% (16%) for the best (upper bound) estimates and total excess morbidities would increase by 22% (35%) for the best (upper bound) estimates. If I-131 were treated exclusively as a particle rather than a gas, an extreme scenario inconsistent with observations, mortalities would increase by 45% (23%) for the best (upper bound) estimates and morbidities would increase by 46% (11%) for the best (upper bound) estimates. If 80% of radioactive I-131 were in the gaseous form, as suggested by EPA RadNet measurements,[50] scaling the numbers above would increase best (upper bound) mortalities by 9% (5%) and increase best (upper bound) morbidities by 9% (2%). Thus, a doubling of the I-131 emission rate and a 4 to 1 gas to particle I-131 ratio would increase best (upper bound) mortalities to 160 (1300) and best (upper bound) morbidities to 240 (2500). Overall, the evacuation radius, emissions profile, and the gas to particle I-131 ratio are all somewhat uncertain, which is why sensitivity analyses were conducted here. Despite these uncertainties, our most confident estimate of radiological health effects to the public determined by this study is provided in Table 2.

Diablo Canyon simulations

Simulations with an identical emission profile to Fukushima were run for hypothetical nuclear releases from the Diablo Canyon Power Plant in California, USA. Two simulations were run, one beginning in March and one beginning in September, to study the impact of location and background meteorology on the health effects of a nuclear accident. Fig. 7 and 8 show the evolution of the I-131 plume for simulations beginning in March and September, respectively. The evolution of the Cs-137 plume for the March and September simulations is shown in ESI Figs. 1 and 2.† Table 3 shows the range in health effects between the two simulations. Projected worldwide mortalities and morbidities for all exposure pathways for the simulation beginning in March were 170 (24–1400) and 250 (38–2300), respectively, and were 140 (11–1600) and 190 (20–2700) for the simulation beginning in September. This results in a total range of 11–1600 mortalities and 20–2700 morbidities over both simulations. In both simulations, a large majority of the total health effect was local to the United States.

Even though the population density of California is roughly one fourth that of Japan, Table 3 indicates that a Diablo Canyon release identical to Fukushima could surpass Fukushima in terms of excess mortalities and morbidities by ~25% for best estimates. This is because the bulk of radioactive emissions at Fukushima were advected westward over the Pacific Ocean, where they decayed or became diluted and removed, whereas in the Diablo Canyon simulations, radioactivity was trapped by an inversion as it was slowly transported along the California coastline over populated regions of Los Angeles and San Diego before it was transported offshore.

Due to the lower latitude storm track in March, radioactivity was dispersed over a larger area in March than in September. In March, fast-moving storms carried radioactivity to the east but

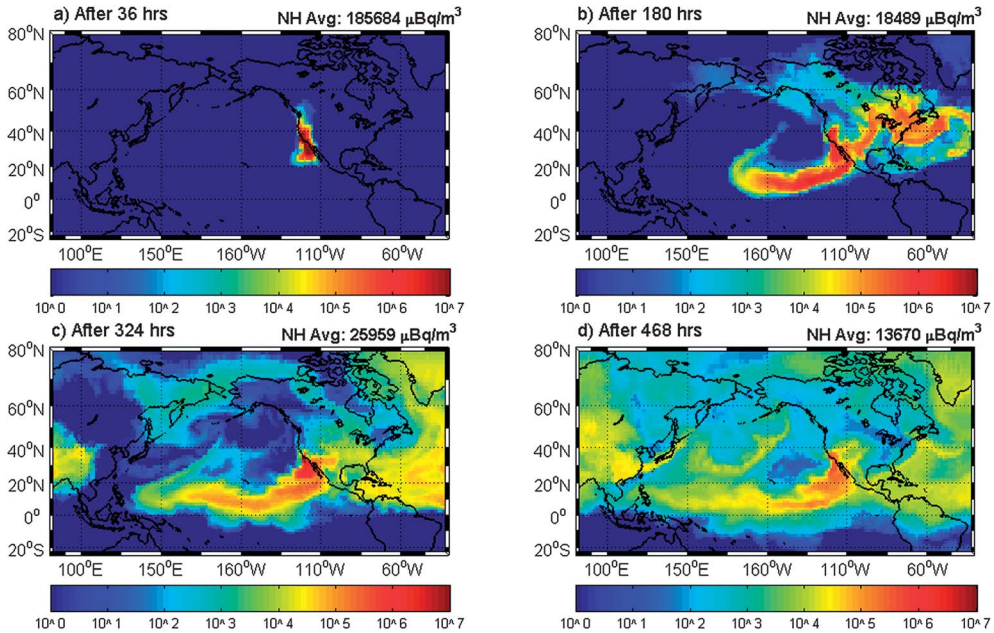

Fig. 7 Modeled near-surface atmospheric worldwide activity concentrations (μBq m^{-3}) of I-131 (a) 36 hours (1.5 days), (b) 180 hours (7.5 days), (c) 324 hours (13.5 days), and (d) 468 hours (19.5 days) into the hypothetical Diablo Canyon simulation beginning on 12 March 2011. Northern Hemisphere (NH) averages noted above each panel are weighted by population.

some radioactivity was also carried to the southwest along the south side of the Pacific High (Fig. 7). In September, the bulk of the radioactivity was transported slowly to the southwest, along the Pacific High. Lower wind speeds hampered the vertical and horizontal dispersion of radionuclides and clear skies prevented wet removal, keeping radioactivity over nearby populated regions for a longer time relative to March (Fig. 8). Fig. 9 shows total deposition of Cs-137 over the month-long March and September simulations. In the March simulation, 51% of total worldwide deposited Cs-137 was deposited over land areas compared with 33% in the September simulation. Population-weighted Cs-137 deposition was also higher in the March simulation by about a factor of four. The higher total Cs-137 deposition over land areas in the March simulation was due to

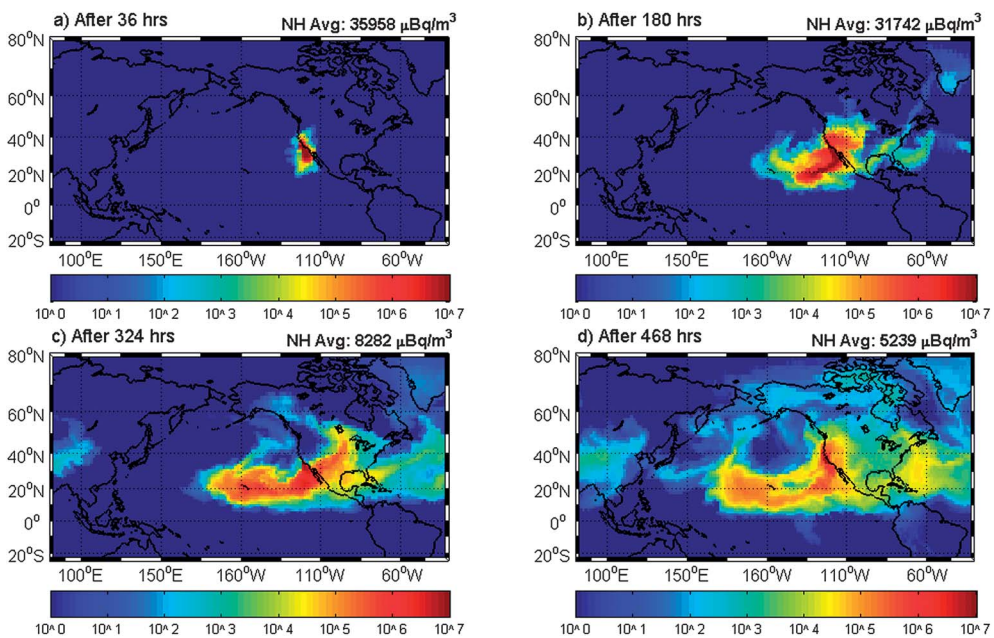

Fig. 8 Modeled near-surface atmospheric worldwide activity concentrations (μBq m^{-3}) of I-131 (a) 36 hours (1.5 days), (b) 180 hours (7.5 days), (c) 324 hours (13.5 days), and (d) 468 hours (19.5 days) into the hypothetical Diablo Canyon simulation beginning on 12 September 2006. Northern Hemisphere (NH) averages noted above each panel are weighted by population.

Table 3 Excess lifetime mortalities and morbidities from radioactivity released from a hypothetical accident at the Diablo Canyon Power Plant by region. Simulations began on 12 March 2011 and 12 September 2006. The middle value provides the average best estimate between the two simulations and the upper and lower values provide the maximum range over both simulations based on uncertainties in the biokinetic, dosimetric, and absorption models used in each simulation. As a result, the "Total" column may not equal the sum of the other columns. The final row provides an estimate of the total health effect including ingestion exposure extrapolated from Chernobyl estimates over both simulations. See Table 2 caption for more information

	Mortalities					Morbidities				
	Inhalation exposure	Ground-level external exposure	Atmospheric external exposure	Total	Percent total after end simulation	Inhalation exposure	Ground-level external exposure	Atmospheric external exposure	Total	Percent total after end simulation
Asia	0.04–1.6–23	0.20–1.3–6.7	0.00–0.03–0.20	0.24–2.9–30	63	0.09–2.6–72	0.30–1.9–9.9	0.00–0.04–0.29	0.39–4.5–82	62
North America	3.1–84–1410	4.1–41–260	0.22–1.2–5.7	10–126–1480	21	6.8–117–2460	5.9–61–382	0.33–1.7–8.5	18–179–2560	22
Europe	0.00–0.23–3.1	0.19–0.82–3.4	0.00–0.00–0.04	0.20–1.1–6.6	69	0.02–0.37–9.6	0.28–1.2–5.0	0.00–0.00–0.05	0.30–1.6–15	68
Africa	0.00–0.57–9.4	0.06–0.33–1.7	0.00–0.00–0.05	0.07–0.90–11	57	0.02–0.95–31	0.09–0.49–2.4	0.00–0.01–0.08	0.11–1.5–33	55
Japan	0.00–0.03–0.40	0.00–0.03–0.21	0.00–0.00–0.00	0.00–0.06–0.61	82	0.00–0.04–1.2	0.00–0.04–0.31	0.00–0.00–0.00	0.00–0.09–1.5	82
China	0.00–0.35–5.2	0.05–0.33–1.8	0.00–0.00–0.05	0.06–0.69–7.1	72	0.02–0.56–15	0.08–0.49–2.7	0.00–0.01–0.07	0.09–1.1–18	72
South Korea	0.00–0.00–0.14	0.00–0.00–0.05	0.00–0.00–0.00	0.00–0.02–0.19	79	0.00–0.02–0.43	0.00–0.01–0.08	0.00–0.00–0.00	0.00–0.03–0.51	79
United States	3.0–78–1310	4.0–41–258	0.21–1.1–5.3	9.4–120–1370	22	6.5–108–2240	5.8–60–379	0.32–1.6–7.8	17–170–2330	22
Mexico	0.14–5.8–102	0.07–0.31–1.4	0.00–0.07–0.46	0.25–6.2–103	6	0.30–8.5–223	0.10–0.46–2.1	0.01–0.11–0.68	0.45–9.1–225	6
Canada	0.00–0.04–0.56	0.02–0.13–0.68	0.00–0.00–0.00	0.02–0.17–1.0	62	0.00–0.06–0.92	0.03–0.19–1.00	0.00–0.00–0.00	0.03–0.24–1.9	61
Worldwide	3.3–86–1420	4.5–44–272	0.24–1.2–5.8	10–131–1490	22	7.4–121–2490	6.6–64–399	0.36–1.8–8.6	19–187–2590	23
	Worldwide total mortality incl. ingestion			11–156–1570		Worldwide total morbidity incl. ingestion			20–224–2700	

Fig. 9 (a) Total wet + dry deposition of Cs-137 (kBq m^{-2}) summed over the one-month simulation for the hypothetical Diablo Canyon nuclear accidents beginning on 12 March 2011 and (b) on 12 September 2006. Northern Hemisphere (NH) averages noted above each panel are weighted by population.

Fig. 10 Time series of Cs-137 ground concentrations (kBq m^{-2}) averaged over the United States for the one-month hypothetical Diablo Canyon simulations beginning on 12 March 2011 and 12 September 2006.

higher wet deposition rates in eastward-moving winter storms. Consequently, ground concentrations of Cs-137 averaged over the United States were also higher in March than in September (Fig. 10).

Inhalation, ground-level external exposure, and ingestion exposure comprised 37%, 40%, and 23%, respectively of best estimate mortalities in the March Diablo Canyon simulation and 78%, 13%, and 8%, respectively of best estimate mortalities in the September simulation. The higher relative inhalation exposure in September was due to lower wet deposition rates and slower winds keeping atmospheric concentrations high in nearby populated areas. The range in the health effect was larger in September due to the higher uncertainty associated with inhalation risk coefficients compared with external exposure risk coefficients. Overall, these results suggest that the geographic

location, as well as the background meteorology and season, may substantially impact the potential health risk from a nuclear accident.

Discussion and conclusions

In 2011, 440 nuclear reactors existed in the world. To date, modest to major radionuclide releases have occurred in almost 1.5 percent of all reactors ever built (Three-Mile Island, 1979; Saint-Laurent, 1980; Chernobyl, 1986; 3 at Fukushima, 2011), suggesting that the risk of a meltdown is not small. This study finds that atmospheric and ground-level radioactivity from a meltdown, even when diluted to the large scale, may have quantifiable health impacts assuming a LNT model of human exposure. Health effects from inhalation, external exposure, and ingestion of radionuclides from the Fukushima accident are estimated to result in 130 (15–1100) cancer-related mortalities and 180 (24–1800) cancer-related morbidities worldwide, taking into account uncertainties associated with the exposure–dose and dose–response models employed. The majority of the health effect is local to Japan and projected mortalities in other countries are much smaller. Sensitivities to the I-131 emission rate and the gas to particle I-131 ratio suggest that total mortalities (morbidities) could increase to 160 (240) for best estimates and 1300 (2500) for upper bound estimates. Yet, due to the substantial uncertainty in the cancer risk from low-dose radiation, the actual number of cancer-related mortalities and morbidities may still fall outside the confidence intervals reported here.

These estimates do not account for the increased radiation risk to the roughly 20 000 workers at the plant in the months following the accident. Recent reports indicate that 146 employees received radiation doses above 100 mSv, the minimum level statistically shown to increase cancer risk.[29,70] Six workers received above 250 mSv, two workers in reactor control rooms received above 600 mSv, and two other workers received skin doses of 2–3 Sv while standing in contaminated water.[70,71] Roughly 400 workers received doses above the annual limit for Japanese workers of 50 mSv.[71] Yet, no acute radiation sickness or acute radiation effects have been reported thus far.[21] One estimate of the total collective exposure is 115 person-Sv.[71] Assuming a LNT model of human exposure where an exposure of 100 mSv increases lifetime cancer risk by 1%,[29] the collective exposure of 115 person-Sv is projected to result in an additional ~12 worker cancers. If the analysis is restricted only to exposures above 100 mSv, the LNT model predicts ~2 to 5 radiological worker cancers depending on the precise amount of radiation received by each grouping.

Health effects due to radiation exposure quantified here occur in addition to other health impacts from the nuclear disaster. Nearly 600 deaths were already certified as "disaster-related" by the 13 municipalities affected by the crisis at Fukushima.[72] These deaths were caused indirectly by fatigue or aggravation of chronic illness due to the disaster, many of which can be attributed to the mandatory evacuation following the accident. We calculated that evacuation procedures after the accident may have potentially reduced radiological mortalities by up to 22%. A 22% reduction translates into a prevention of 3–245 mortalities with a best estimate of 28 mortalities. Interestingly, even the upper bound projection of the lives saved from the evacuation is lower than the number of deaths already caused by the evacuation itself.

The Chernobyl disaster has illustrated that long-term psychological effects, including depression, anxiety, fear, and unexplained physical symptoms, may increase following a nuclear accident.[16,73,74] Similar psychological effects are likely to occur in evacuees after Fukushima. Widespread mistrust of the Japanese government following the accident may also have contributed to these symptoms.[22] In addition to the physical and mental health effects discussed here, the accident also resulted in economic losses in the billions of dollars due to cleanup costs and reduced economic activity in radioactive areas around Fukushima.[22]

Our results are relatively consistent with an estimate of the local health effects from Fukushima. von Hippel [2011] estimated that 1 million people live in areas with more than 1 curie per km^2 deposition of Cs-137, and that people living in these areas were subject to a 0.1% increase in cancer risk, resulting in 1000 excess cancers.[3,75,76] Our results are somewhat lower than those of von Hippel [2011] due to the lower relative risk per unit of radioactivity assumed in our study. Total Cs-137 wet + dry deposition in the grid cell containing Fukushima (population ~2 million) was 65 kBq m^{-2}, above the threshold of 1 curie per km^2 (37 kBq m^{-2}), but we estimate only 66 (7–680) excess mortalities in this grid cell. Our study accounted for time-dependent and location-dependent emission, transport, removal, and decay of radioactivity in the atmosphere and on the ground, which von Hippel [2011] did not, and still our results are relatively consistent. A study by the Institut de Radioprotection et de Sûreté Nucléaire (IRSN) estimated a population of 21 100 receiving >16 mSv, 3100 receiving >50 mSv, and 2200 receiving 100–500 mSv near Fukushima.[75] Assuming a LNT model where an exposure of 100 mSv increases lifetime cancer risk by 1%,[29] the collective exposure estimated by IRSN is projected to result in ~70–250 excess cancers depending on the precise amount of radiation received by each grouping. Our estimate of ~180 excess cancers is within this range.

Several studies have attributed several thousand cancer mortalities to radiation released from Chernobyl, including nearly 30 workers that died of acute radiation sickness.[16,19] To date, nearly 6000 thyroid cancers have been detected in contaminated regions, many from I-131 exposure from the accident.[16] Studies estimate an additional 10 000–40 000 cancers over the next several decades.[18,19,29] Why is the number of cancer morbidities predicted from Fukushima substantially less than the number of morbidities predicted from Chernobyl? Firstly, total I-131 and Cs-137 radiation released from Fukushima is roughly an order of magnitude lower than the total radiation released from Chernobyl.[3,47] In comparison, the total amount of I-131 and Cs-137 released from the Three Mile Island accident was 1/100 000 and 1/100 000 000 000 that of Fukushima, respectively, suggesting a total excess cancer burden of near zero associated with the Three Mile Island accident.[40] Secondly, a majority of the radioactivity from Fukushima was deposited over the Pacific Ocean (~81% calculated here). After Chernobyl, in comparison, a large majority of the radiation was deposited over land areas in Europe and Asia and <10% was deposited over oceans.[20,77] Lastly, preventive actions taken by the Japanese

government after Fukushima may have reduced radiological health impacts substantially. Five days after the accident, stable iodine tablets were distributed to people in evacuation centers under 40 years of age to prevent I-131 uptake by the thyroid.[61] In addition, the government prohibited cultivation of all vegetables, grain, milk, and other food products containing more than 2000 Bq kg^{-1} radioactive iodine and 500 Bq kg^{-1} radioactive cesium.[22,23] About 1000 children evacuated from the 20 km zone around the plant were tested for I-131 exposure at the end of March, and no child revealed thyroid dose rates above 0.07 μSv h^{-1}, suggesting that high dose rates did not occur in the group.[61] In contrast, millions of children ingested contaminated milk in the countries of Belarus, Ukraine, and the Russian Federation after Chernobyl, resulting in mean thyroid doses between 100 and 5000 mGy and thousands of cases of thyroid cancer.[76] Additional factors resulting in the differences between dose rates following Chernobyl and Fukushima are detailed by Boice [2011].[21]

A hypothetical accident at the Diablo Canyon Nuclear Power Plant, in California, USA was simulated to analyze the influence of location and background meteorology on health effects resulting from a nuclear accident. Two simulations, one beginning in March and one beginning in September, were run with identical emissions to the Fukushima accident. We estimate total excess mortalities of 160 (11–1600) and morbidities of 220 (20–2700) over both Diablo Canyon simulations. Similar to Fukushima, a large majority of the health effect is local. Averaged over both Diablo Canyon simulations, we find ~25% more mortalities compared with the Fukushima simulation for best estimates. The larger projected health effect occurs despite a lower local population density in California relative to Japan, and is attributed to differences in meteorological conditions between the two simulated accidents. In the Diablo Canyon simulations, radiation was capped in a shallow layer near the surface and was slowly advected over nearby populated areas whereas in the Fukushima simulation, much of the radiation was quickly advected offshore where it was diluted and removed.

We also find a difference in the age of the affected population between the Fukushima and Diablo Canyon simulations. In the Fukushima simulation, 36% of mortalities occur in people 0–20 years of age and 19% of mortalities occur in people 60 and older. Averaged over both Diablo Canyon simulations, 50% of mortalities occur in people 0–20 years of age and 10% of mortalities occur in people 60+. The difference is due to Japan's aging population – Japan has the highest proportion of elderly citizens compared to any other country in the world, resulting in the higher percentage of mortalities in the Fukushima simulation for people 60+.[78] In general, however, cancer risks are greater for younger ages, resulting in a higher cancer incidence rate in the 0–20 population compared with the 60+ population even though the 0–20 population is about 40% lower than the 60+ population in Japan.[62] In both simulations, about 45% of the mortalities occurred in males and 55% occurred in females. The higher number of cancers in females is largely because there are more females than males in the populations of both Japan and the United States integrated over all age groups since women generally live longer than men.[63]

The future of the nuclear energy industry relies on the contention that nuclear energy is safe. Here, we find that the Fukushima nuclear accident may cause nontrivial cancer mortality and morbidity assuming an LNT model of human exposure, and hypothetical accidents at the Diablo Canyon Power Plant of comparable magnitude may cause similar health effects despite having one fourth the local population density as Fukushima. The number of projected mortalities, however, is still considerably smaller than the nearly 20 000 mortalities from the Tōhoku earthquake and tsunami[79] and is also smaller than the estimated number of projected mortalities from the Chernobyl nuclear accident.[16,18,19,76] Nevertheless, long-term cancer risk studies should be conducted in Japan to compare with the estimates developed here as well as with future modeling studies of the health effects from Fukushima.[36] The risks and consequences of a meltdown must be considered along with other impacts, risks, costs, and benefits of nuclear power, discussed elsewhere, in comparison with other electric power sources in deciding the future direction of worldwide energy policy.

Acknowledgements

We thank Lt. Col. John Smith at the United States Air Force for providing access to U.S. CTBTO data. We also thank Dr Yu Morino at the Japanese Center for Regional Environmental Research for providing access to radionuclide deposition measurements. Partial support came from a NASA Earth and Space Science Fellowship, the Department of the Army Center at Stanford University, and U.S. Environmental Protection Agency grant RD-83337101-O.

References

1 T. Takemura, H. Nakamura and T. Nakajima, *EOS, Trans. Am. Geophys. Union*, 2011, **92**, 397–398.
2 Tokyo Electric Power Company, Impact to TEPCO's Facilities due to Miyagiken-Oki Earthquake (as of 5 PM), 2011, http://www.tepco.co.jp/en/press/corp-com/release/11031223-e.html.
3 F. N. von Hippel, *Bulletin of the Atomic Scientists*, 2011, **67**, 27–36.
4 O. Masson, A. Baeza, J. Bieringer, K. Brudecki, S. Bucci, M. Cappai, F. P. Carvalho, O. Connan, C. Cosma, A. Dalheimer, D. Didier, G. Depuydt, L. E. De Geer, A. De Vismes, L. Gini, F. Groppi, K. Gudnason, R. Gurriaran, D. Hainz, O. Halldórsson, D. Hammond, O. Hanley, K. Holeý, Z. Homoki, A. Ioannidou, K. Isajenko, M. Jankovic, C. Katzlberger, M. Kettunen, R. Kierepko, R. Kontro, P. J. M. Kwakman, M. Lecomte, L. Leon Vintro, A. P. Leppänen, B. Lind, G. Lujaniene, P. Mc Ginnity, C. M. Mahon, H. Malá, S. Manenti, M. Manolopoulou, A. Mattila, A. Mauring, J. W. Mietelski, B. Møller, S. P. Nielsen, J. Nikolic, R. M. W. Overwater, S. E. Pálsson, C. Papastefanou, I. Penev, M. K. Pham, P. P. Povinec, H. Ramebäck, M. C. Reis, W. Ringer, A. Rodriguez, P. Rulík, P. R. J. Saey, V. Samsonov, C. Schlosser, G. Sgorbati, B. V. Silobritiene, C. Söderström, R. Sogni, L. Solier, M. Sonck, G. Steinhauser, T. Steinkopff, P. Steinmann, S. Stoulos, I. Sýkora, D. Todorovic, N. Tooloutalaie, L. Tositti, J. Tschiersch, A. Ugron, E. Vagena, A. Vargas, H. Wershofen and O. Zhukova, *Environ. Sci. Technol.*, 2011, **45**, 7670–7677.
5 J. Diaz Leon, J. Kaspar, A. Knecht, M. L. Miller, R. G. H. Robertson and A. G. Schubert, *J. Environ. Radioact.*, 2011, **102**, 1032–1038.
6 G. Brumfiel, Fukushima reaches cold shutdown, *Nature|From The Blog*, http://www.nature.com/news/fukushima-reaches-cold-shutdown-1.9674, 16 December 2011.
7 N. Kinoshita, K. Sueki, K. Sasa, J.-I. Kitagawa, S. Ikarashi, T. Nishimura, Y.-S. Wong, Y. Satou, K. Handa, T. Takahashi, M. Sato and T. Yamagata, *Proc. Natl. Acad. Sci. U. S. A.*, 2011, **108**, 19526–19529.
8 T. Yasunari, A. Stohl, R. Hayano, J. Burkhart, S. Eckhardt and T. Yasunari, *Proc. Natl. Acad. Sci. U. S. A.*, 2011, **108**, 19530–19534.

9 A. Stohl, P. Seibert, G. Wotawa, D. Arnold, J. F. Burkhart, S. Eckhardt, C. Tapia, A. Vargas and T. J. Yasunari, *Atmos. Chem. Phys. Discuss.*, 2011, **11**, 28319–28394.
10 Y. Morino, T. Ohara and M. Nishizawa, *Geophys. Res. Lett.*, 2011, **38**, L00G11.
11 G. Sugiyama, J. Nasstrom, B. Pobanz, K. Foster, M. Simpson, P. Vogt, F. Aluzzi and S. Homann, *Health Phys.*, 2012, **102**, 493–508.
12 M. Z. Jacobson, *J. Geophys. Res.*, 2001, **106**, 5385–5401.
13 M. Z. Jacobson, *J. Geophys. Res.*, 2010, **115**, D14209.
14 F. Medici, *Radiat. Phys. Chem.*, 2001, **61**, 689–690.
15 Ministry of Education/Culture/Sports/Science/Technology, Reading of radioactivity level in fallout by prefecture, 2011, http://radioactivity.mext.go.jp/en/.
16 UNSCEAR, *Annex D: Health Effects Due to Radiation from the Chernobyl Accident*, United Nations Scientific Committee on the Effects of Atomic Radiation, 2008, Report ISBN-13: 978-92-1-142280-1, http://www.unscear.org/docs/reports/2008/11-80076_Report_2008_Annex_D.pdf.
17 A. Albergel, D. Martin, B. Strauss and J.-M. Gros, *Atmos. Environ.*, 1988, **22**, 2431–2444.
18 L. Anspaugh, R. Catlin and M. Goldman, *Science*, 1988, **242**, 1513–1519.
19 E. Cardis, D. Krewski, M. Boniol, V. Drozdovitch, S. C. Darby, E. S. Gilbert, S. Akiba, J. Benichou, J. Ferlay, S. Gandini, C. Hill, G. Howe, A. Kesminiene, M. Moser, M. Sanchez, H. Storm, L. Voisin and P. Boyle, *Int. J. Cancer*, 2006, **119**, 1224–1235.
20 H. Hass, M. Memmesheimer, H. Geiß, H. J. Jakobs, M. Laube and A. Ebel, *Atmos. Environ., Part A*, 1990, **24**, 673–692.
21 J. D. Boice, *J. Radiol. Prot.*, 2012, **32**, N33–N40.
22 G. Brumfiel and I. Fuyuno, *Nature*, 2012, **483**, 138–140.
23 K. Akahane, S. Yonai, S. Fukuda, N. Miyahara, H. Yasuda, K. Iwaoka, M. Matsumoto, A. Fukumura and M. Akashi, *Environmentalist*, 2012, **32**, 136–143.
24 R. Adams, As Fukushima gets moved from 5 to 7 remember that 0 (deaths) is still an applicable number, *Atomic Insights*, 12 April 2011, http://atomicinsights.com/2011/04/as-fukushima-gets-moved-from-5-to-7-remember-that-0-deaths-is-still-an-applicable-number.html.
25 F. Dahl, U.N. expert sees no serious Fukushima health impact, *Reuters*, 18 April 2011, http://www.reuters.com/article/2011/04/06/us-japan-nuclear-health-idUSTRE7354H920110406.
26 CDC, *Radiation Emergencies: Radioisotope Brief: I-131, Cs-137*, Department of Health and Human Services/Centers for Disease Control and Prevention, 2005, http://www.bt.cdc.gov/radiation/isotopes/pdf/iodine.pdf, http://www.bt.cdc.gov/radiation/isotopes/pdf/cesium.pdf.
27 K. F. Eckerman, R. W. Leggett, C. B. Nelson, J. S. Puskin and A. C. B. Richardson, Federal Guidance Report No. 13, *Cancer Risk Coefficients for Environmental Exposure to Radionuclides*, Office of Radiation and Indoor Air/Environmental Protection Agency/Oak Ridge National Laboratory, 1999, Report EPA 402-R-99–001.
28 ICRP, *Low-Dose Extrapolation of Radiation-Related Cancer Risk – ICRP Publication 99*, International Commission on Radiological Protection, 2005.
29 NRC, *Health Risks from Exposure to Low Levels of Ionizing Radiation: Beir VII Phase 2*, U.S. National Research Council, 2006, Report ISBN: 0-309-09156-5.
30 UNSCEAR, *Summary of Low-Dose Radiation Effects on Health*, United Nations Scientific Committee on the Effects of Atomic Radiation, 2010, Report ISBN 978-92-1-642010-9, http://www.unscear.org/docs/reports/2010/UNSCEAR_2010_Report_M.pdf.
31 J. M. Cuttler, *Dose-Response*, 2010, **8**, 378–383.
32 M. Goldman, *Science*, 1996, **271**, 1821–1822.
33 E. Calabrese, *Proc. Natl. Acad. Sci. U. S. A.*, 2011, **108**, 19447–19448.
34 J. A. Siegel and M. G. Stabin, *Health Phys.*, 2012, **102**, 90–99.
35 M. Tubiana, L. E. Feinendegen, C. C. Yang and J. M. Kaminski, *Radiology*, 2009, **251**, 13–22.
36 D. Normile, *Science*, 2011, **332**, 908–910.
37 E. J. Calabrese, *Toxicol. Appl. Pharmacol.*, 2004, **197**, 125–136.
38 F. O. Hoffman, D. C. Kocher and A. I. Apostoaei, *Health Phys.*, 2012, **102**, 591–592.
39 NRC, *Fact Sheet on Biological Effects of Radiation*, U.S. Nuclear Regulatory Commission, 2011, http://www.nrc.gov/reading-rm/doc-collections/fact-sheets/bio-effects-radiation.html.
40 H. Behling and J. E. Hildebrand, *Radiation and Health Effects – A Report on the TMI-2 Accident and Related Health Studies*, GPU Nuclear Corporation, 1986, http://www.threemileisland.org/downloads/224.pdf.
41 J. Upton, Seismic Uncertainty at Diablo Canyon, *The Bay Citizen*, 18 March 2011, http://www.baycitizen.org/pge/story/diablo-canyon/.
42 E. S. Lyman, *Bulletin of the Atomic Scientists*, 2011, **67**, 47–54.
43 NRC, Diablo Canyon Power Plant – NRC Temporary Instruction 2515/183 Inspection Report 05000275/2011006 and 05000323/2011006, 2011, http://pbadupws.nrc.gov/docs/ML1113/ML11133A310.pdf.
44 Zentral Anstalt für Meteorologie and Geodynamik, *Aktuelle Lage nach Unfall in Fukushima*, (Update: 1, April 2011, 12:00), http://www.zamg.ac.at/aktuell/index.php?seite=1&artikel=ZAMG_2011-04-01GMT11:25, accessed 4 April 2011.
45 Nuclear and Industrial Safety Agency, INES (the International Nuclear and Radiological Event Scale) Rating on the Events in Fukushima Daiichi Nuclear Power Station by the Tohoku District – off the Pacific Ocean Earthquake, Ministry of Economy/Trade/Industry, 2011, http://www.nisa.meti.go.jp/english/files/en20110412-4.pdf.
46 M. Chino, H. Nakayama, H. Nagai, H. Terada, G. Katata and H. Yamazawa, *J. Nucl. Sci. Technol.*, 2011, **48**, 1129–1134.
47 V. Winiarek, M. Bocquet, O. Saunier and A. Mathieu, *J. Geophys. Res.*, 2012, **117**, D05122.
48 S. Biegalski, O. Ezekoye, M. Pickering, J. Peña and S. Waye, *J. Radioanal. Nucl. Chem.*, 2008, **276**, 441–445.
49 D. L. Williams, *Presented in Part at the 7th International Conference on Nuclear Engineering*, Tokyo, Japan, 1999.
50 K. F. Chen, R. L. Buckley, R. Kurzeja, L. O'Steen and S. R. Salaymeh, *Optimizing Radiological Monitor Siting Over the Continental United States*, U.S. Department of Energy, 2007, Report WSRC-STI-2007–00621.
51 B. Sportisse, *Atmos. Environ.*, 2007, **41**, 2683–2698.
52 C. J. Walcek, *J. Geophys. Res.*, 2000, **105**, 9335–9348.
53 M. Z. Jacobson, *Fundamentals of Atmospheric Modeling*, Cambridge University Press, Cambridge, 2005.
54 R. Sander, *Compilation of Henry's Law Constants for Inorganic and Organic Species of Potential Importance in Environmental Chemistry*, Max-Planck Institute of Chemistry, 1999, http://www.ceset.unicamp.br/~mariaacm/ST405/Lei%2520de%2520Henry.pdf.
55 M. Z. Jacobson, *J. Geophys. Res.*, 2002, **107**, 4366.
56 J. F. Stara and R. G. Thomas, *The Tissue Distribution and Excretion of Cesium-137 Following Inhalation: Preliminary Data for Rats*, Lovelace Foundation for Medical Education and Research/Atomic Energy Commission, 1963.
57 M.-D. Dorrian, *Radiat. Prot. Dosim.*, 1997, **69**, 117–132.
58 M. Lederer, J. M. Hollander and I. Perlmann, *Table of Isotopes*, Wiley and Sons, New York, 1967.
59 C. F. Baes, R. D. Sharp, A. L. Sjoreen and R. W. Shor, *A Review and Analysis of Parameters for Assessing Transport of Environmentally Released Radionuclides Through Agriculture*, Oak Ridge NationalLaboratory, 1984, Report ORNL-5786, http://homer.ornl.gov/baes/documents/ornl5786.pdf.
60 Global Forecast System (GFS) – 1 deg × 1 deg Reanalysis Fields, NOAA National Operational Model Archive and Distribution System, 2011, http://nomads.ncdc.noaa.gov/data/gfs-avn-hi/.
61 R. Wakeford, *J. Radiol. Prot.*, 2011, **31**, 167–176.
62 *Dose and Risk Calculation (DCAL) Software*, Oak Ridge National Laboratory/Environmental Protection Agency, 2006, http://www.epa.gov/radiation/assessment/dcal.html.
63 *International Data Base*, U.S. Census Bureau, 2011, http://www.census.gov/population/international/data/idb/.
64 M. Z. Jacobson, *Environ. Sci. Technol.*, 2010, **44**, 2497–2502.
65 B. N. Price and B. Jayaraman, *Indoor Exposure to Radiation in the Case of an Outdoor Release*, Lawrence Livermore National Laboratory, 2006, Report LBNL-60662, http://e-reports-ext.llnl.gov/pdf/335508.pdf.
66 P. C. Novelli, P. M. Lang, K. A. Masarie, D. F. Hurst, R. Myers and J. W. Elkins, *J. Geophys. Res.*, 1999, **104**, 30427–30444.
67 T. S. Rhee, C. A. M. Brenninkmeijer and T. Rockmann, *Atmos. Chem. Phys.*, 2006, **6**, 1611–1625.
68 *Contribution of Tropical Ecosystems to the Global Budgets of Trace Gases, Especially CH_4, H_2, CO, and N_2O*, ed. W. Seiler and R. Conrad, John Wiley and Sons, New York, 1987.

69 CBC News World, *Japan Ignored Own Radiation Forecasts*, The Associated Press, 9 August 2011, http://www.cbc.ca/news/world/story/2011/08/09/japan-nuclear-crisis-reactor.html.
70 G. Brumfiel, *Nature|News*, 2012, **485**, 423–424.
71 American Nuclear Society, *Fukushima Daiichi – ANS Committee Report*, American Nuclear Society, 2012, http://fukushima.ans.org/report/Fukushima_report.pdf.
72 The Yomiuri Shimbun, 573 deaths 'related to nuclear crisis', The Yomiuri Shimbun, 5 Febraury 2012, http://www.yomiuri.co.jp/dy/national/T120204003191.htm.
73 E. J. Bromet, J. M. Havenaar and L. T. Guey, *Clin. Oncol.*, 2011, **23**, 297–305.
74 E. J. Bromet, *J. Radiol. Prot.*, 2012, **32**, N71–N75.
75 IRSN, *Assessment on the 66th Day of Projected External Doses for Populations Living in the North-West Fallout Zone of the Fukushima Nuclear Accident*, Institut de Radioprotection et de Sûreté Nucléaire, 2011, Report DRPH/2011-10, http://www.irsn.fr/EN/news/Documents/IRSN-Fukushima-Report-DRPH-23052011.pdf.
76 E. Cardis, G. Howe, E. Ron, V. Bebeshko, T. Bogdanova, A. Bouville, Z. Carr, V. Chumak, S. Davis, Y. Demidchik, V. Drozdovitch, N. Gentner, N. Gudzenko, M. Hatch, V. Ivanov, P. Jacob, E. Kapitonova, Y. Kenigsberg, A. Kesminiene, K. J. Kopecky, V. Kryuchkov, A. Loos, A. Pinchera, C. Reiners, M. Repacholi, Y. Shibata, R. E. Shore, G. Thomas, M. Tirmarche, S. Yamashita and I. Zvonova, *J. Radiol. Prot.*, 2006, **26**, 127–140.
77 REM, *Atlas on the Caesium Deposition Across Europe After the Chernobyl Accident*, European Commission Joint Research Centre – Radioactivity Environmental Monitoring, 1998, Report ISBN 92-828-3140-X, http://rem.jrc.ec.europa.eu/RemWeb/pastprojects/Atlas.aspx.
78 World Briefing|Asia, *Japan: Most Elderly Nation*, New York Times, 1 July 2006, http://query.nytimes.com/gst/fullpage.html?res=9C04EEDC1530F932A35754C0A9609C8B63.
79 J. McCurry, Japan quake death toll passes 18 000, The Guardian, Date: 21 March 2011, http://www.guardian.co.uk/world/2011/mar/21/japan-earthquake-death-toll-18000.